

Consider for Best Student Paper Award

Model-Free Control for Quadrotor Attitude via Tent Map-Based Pigeon-Inspired Optimization

Yang Yuan¹, Haibin Duan², *Senior Member, IEEE*, Chen Wei³

Abstract—The attitude control problem of the quadrotor in the presence of disturbance and model uncertainty is studied in this paper. Firstly, a first-order filter is applied to generate the desired derivate of the reference signal. Then, a model-free adaptive attitude controller is designed for the condition that model parameters are not available. The discrete equation of the angular velocity is obtained by using the compact form dynamic linearization method, and the cascade controller is established based on the continuous kinematics and discrete dynamics. In addition, tent map-based pigeon-inspired optimization is designed to optimize the parameters of the filter and controller. Compared with original pigeon-inspired optimization, the premature problem can be effectively contained. Finally, the simulation results demonstrate the feasibility of the model-free attitude controller and the advantages of the Tent map-based pigeon-inspired optimization.

I. INTRODUCTION

Quadrotor has been utilized in many fields, such as aerial photography and terrain exploration, for its advantages of low cost, simple operation and strong capability [1-2]. Due to the underactuated characteristics of the quadrotor, position and attitude are generally controlled in cascades. The rapidity and accuracy of attitude control are the basis of accurate position control. However, high nonlinearity, external disturbance and model uncertainty make the attitude control a challenging task.

Sliding mode control (SMC) [3], differential-flatness technique [4], backstepping control [5], and many other technologies have been applied for quadrotor attitude tracking. Attitude tracking performance is guaranteed by utilizing dynamic surface control method and prescribed performance function in [6]. Fast terminal SMC and model predictive control are applied to the attitude control in [7,8], where the uncertainties and disturbances are estimated with on-

line updating rules. Considering the actuator faults, a robust finite-time controller is designed by using mixed H-infinite controller and Lyapunov-Krasovskii functional for the quadrotor attitude [9]. The actuator saturation is also included in the investigation for the quadrotor attitude, and non-fragile fault alarm technique is developed for the fault condition [10]. However, a nominal model with some known model information is necessary in above works, the case where model parameters are completely unknown still cannot be well solved.

Proportion-integration-differentiation controller has the advantage of not using prior information of the model, while the control performance is weakened by external disturbance. Model-free adaptive control (MFAC) is an effective technique without using model parameters [11], which has been applied in unmanned aerial vehicles (UAVs) [12], autonomous cars [13], wastewater treatment process [14], etc. MFAC based on forecasting method is utilized to handle the unknown model for the spacecraft attitude control in [15]. SMC-based MFAC is studied for autonomous surface vehicles (ASVs) tracking, and a data-driven observer is used for the compensation in [16]. Thus, MFAC is utilized for the quadrotor attitude control problem in this paper.

For a better control performance, pigeon-inspired optimization (PIO) is selected as the tool to obtain the optimal controller gain [17], which has the advantages of fast convergence and effective search performance. However, PIO suffers the problem that falls into the local optimum. A lot of variants have been developed for the problem, such as paired coevolution (PIO) [1], Cauchy mutation PIO [18]. In this paper, Tent map-based PIO (TMPIO) is developed to search the optimal filter parameters and controller gain.

The main contributions of the article are summarized in the following three aspects:

- (1) The quadrotor attitude model with unknown parameters and external disturbances is transformed into a continuous-discrete form for the data-driven controller design.
- (2) Model-free controller is designed for the continuous-discrete attitude model. A differentiation term is included in the MFAC cost index design for the rapidity and stability.
- (3) TMPIO is proposed to alleviate the premature convergence of PIO in the paper, where two stages of PIO are fused into one operator in TMPIO, and Tent map is utilized to generate the coefficient of the landmark operator to escape the local optimum.

*This work was partially supported by Science and Technology Innovation 2030-Key Project of "New Generation Artificial Intelligence" under grant 2018AAA0102403, National Natural Science Foundation of China under grant U20B2071, T2121003 and U1913602. (Corresponding author: Haibin Duan).

¹Yang Yuan is with State Key Laboratory of Virtual Reality Technology and Systems, School of Automation Science and Electrical Engineering, Beihang University, Beijing 100083, China yyuan@buaa.edu.cn

²Haibin Duan is with State Key Laboratory of Virtual Reality Technology and Systems, School of Automation Science and Electrical Engineering, Beihang University, Beijing 100083, China, and Virtual Reality Fundamental Research Laboratory, Department of Mathematics and Theories, Peng Cheng Laboratory, Shenzhen, 518000, China hbduan@buaa.edu.cn

³Chen Wei is with State Key Laboratory of Virtual Reality Technology and Systems, School of Automation Science and Electrical Engineering, Beihang University, Beijing 100083, China weichen@buaa.edu.cn

The remainder of the paper is organized as follows. In Section 2, attitude model and preliminaries are presented. Section 3 gives the main results of the paper. Simulation results are shown in Section 4. Section 5 concludes the paper.

II. ATTITUDE MODEL AND PRELIMINARIES

A. Attitude Model

The attitude model of the quadrotor is described as [1]

$$\begin{cases} \dot{\eta} = R_r \Omega \\ J\dot{\Omega} = -\Omega \times (J\Omega) + \tau + d \end{cases} \quad (1)$$

where η and Ω are respectively the Euler angle vector and the angular velocity vector, τ is the torque of the UAV, J implies the inertial moment matrix, d represents the the external disturbanceof the model, R_r is the attitude transformation matrix.

B. Preliminaries

Notation 1: $\text{sgn}()$ means the sign function. For $\varphi \in \mathbb{R}$ and $\omega \in \mathbb{R}$, $\text{sig}^\omega(\varphi) = \text{sgn}(\varphi)|\varphi|^\omega$, where $|\varphi|$ represents the absolute value of φ . For $y \in \mathbb{R}^n$, $\text{sig}^\omega(y) = [\text{sig}^\omega(y_1), \dots, \text{sig}^\omega(y_n)]^T$. $\|y\|$ implies the Euclidean norm of y .

Lemma 1 [19]: Considering the system $\dot{\vartheta} = \Upsilon(\vartheta)$, $\Upsilon(0) = 0$, $\vartheta \in \mathbb{R}^n$, where $\Upsilon(\vartheta)$ is continuous in the neighborhood U of the origin. If the Lyapunov function $\Psi(\vartheta)$ can be established on U , and $\dot{\Psi}(\vartheta) + \iota\Psi^\xi(\vartheta) + \kappa\Psi^\zeta(\vartheta) + \varrho \leq 0$ is satisfied, where ι , κ , and ϱ are positive constant, $0 < \xi < 1$, $\zeta > 1$, the signal is bound in a fixed time.

III. MAIN RESULTS

A. First-Order Filter

The reference attitude signal is notes as η_r . Due to the first-order differential of η_r is utilized in the designed controller, a first-order filter is used to generate the reference signal, described as [19]

$$\dot{\eta}_d = -\gamma_1 \text{sig}^{\chi_1}(\eta_d - \eta_r) - \gamma_2 \text{sig}^{\chi_2}(\eta_d - \eta_r) \quad (2)$$

where η_d represents the desired attitude signal, $\gamma_1, \gamma_2, \chi_1 \in (0, 1)$, and $\chi_2 \in (1, 2)$ are positive scalars to be designed.

Assumption 1: The derivative of η_r is bounded by $\|\dot{\eta}_r\| \leq L$, where L is an unknown constant.

Denote the filter error as $\eta_e = \eta_d - \eta_r$, and select the Lyapunov function as $\Psi_\eta = \frac{1}{2}\eta_e^T \eta_e$. The differential of Ψ_η is calculated as

$$\begin{aligned} \dot{\Psi}_\eta &= \eta_e^T \dot{\eta}_e \\ &= \eta_e^T (-\gamma_1 \text{sig}^{\chi_1}(\eta_d - \eta_r) - \gamma_2 \text{sig}^{\chi_2}(\eta_d - \eta_r) - \dot{\eta}_r) \quad (3) \\ &= -\gamma_1 \eta_e^T \text{sig}^{\chi_1}(\eta_e) - \gamma_2 \eta_e^T \text{sig}^{\chi_2}(\eta_e) - \eta_e^T \dot{\eta}_r \end{aligned}$$

Considering the following inequality,

$$-\eta_e^T \dot{\eta}_r \leq \frac{1}{2}\eta_e^T \eta_e + \frac{1}{2}L^2 \quad (4)$$

Substituting (4) into (3), it is obtained that

$$\begin{aligned} \dot{\Psi}_\eta &\leq -\gamma_1 \eta_e^T \text{sig}^{\chi_1}(\eta_e) - \gamma_2 \eta_e^T \text{sig}^{\chi_2}(\eta_e) \\ &\quad + \frac{1}{2}\eta_e^T \eta_e + \frac{1}{2}L^2 \\ &\leq -2^{(\chi_1+1)/2}\gamma_1 \Psi_\eta^{(\chi_1+1)/2} - 2^{(\chi_2+1)/2}\gamma_2 \Psi_\eta^{(\chi_2+1)/2} \quad (5) \\ &\quad + \Psi_\eta + \frac{1}{2}L^2 \end{aligned}$$

Let $2^{(\chi_1+1)/2}\gamma_1 > 1$ and $2^{(\chi_2+1)/2}\gamma_2 > 1$. If $\Psi_\eta < 1$, it can be deduced that

$$\begin{aligned} \dot{\Psi}_\eta &\leq -\left(2^{(\chi_1+1)/2}\gamma_1 - 1\right) \Psi_\eta^{(\chi_1+1)/2} \\ &\quad - 2^{(\chi_2+1)/2}\gamma_2 \Psi_\eta^{(\chi_2+1)/2} + \frac{1}{2}L^2 \quad (6) \end{aligned}$$

If $\Psi_\eta \geq 1$, it can be obtained that

$$\begin{aligned} \dot{\Psi}_\eta &\leq -2^{(\chi_1+1)/2}\gamma_1 \Psi_\eta^{(\chi_1+1)/2} \\ &\quad - \left(2^{(\chi_2+1)/2}\gamma_2 - 1\right) \Psi_\eta^{(\chi_2+1)/2} + \frac{1}{2}L^2 \quad (7) \end{aligned}$$

Thus, combining the results of (6) and (7), the filter error η_e will approach the neighbor of the origin in a fixed time by Lemma 1.

B. Controller Design

Redefine the attitude model in (1) as follows:

$$\begin{cases} \dot{s}_1(t) = s_2(t) \\ \dot{s}_2(t) = \dot{R}_r \Omega + R_r J^{-1}(-\Omega \times (J\Omega) + \tau + d) \end{cases} \quad (8)$$

where $s_1(t) = \eta$, $s_2(t) = R_r \Omega$.

Considering the model parameters are not available, the data-driven MFAC method is applied to the angular velocity loop. Utilizing the dynamic linearization method, an equivalent discrete model of the kinetics in (8) can be reformulated as

$$s_2(\sigma + 1) = s_2(\sigma) + \Upsilon(s_2(k\sigma), \tau(\sigma), d(\sigma)) \quad (9)$$

Thus, the continuous-discrete model can be obtained as

$$\begin{cases} \dot{s}_1(t, \sigma) = s_2(\sigma) \\ s_2(\sigma + 1) = s_2(\sigma) + \Upsilon(s_2(\sigma), \tau(\sigma), d(\sigma)) \end{cases} \quad (10)$$

where $s_1(t, \sigma)$ means the s_1 value in the time region $t \in [\sigma T, (\sigma + 1)T)$, T represents the fixed sampling interval.

Step 1: Design the continuous controller for the first equation in (10). s_1 and s_2 are utilized to represent $s_1(t, \sigma)$ and $s_1(t, \sigma)$ for simplicity.

Define the attitude tracking error as $\varepsilon_1 = s_1 - \eta_d$, of which the differential is governed by

$$\begin{aligned} \dot{\varepsilon}_1 &= \dot{s}_1 - \dot{\eta}_d \\ &= s_2 - \dot{\eta}_d \\ &= (s_2 - \alpha_1) + \alpha_1 - \dot{\eta}_d \end{aligned} \quad (11)$$

where α_1 is the virtual controller.

Design the controller α_1 as

$$\alpha_1 = -c_1 \varepsilon_1 + \dot{\eta}_d \quad (12)$$

where c_1 is a positive scalar.

Select the Lyapunov function as $\Psi_1 = \frac{1}{2}\varepsilon_1^T \varepsilon_1$, and the derivate of Ψ_1 yields that

$$\begin{aligned}\dot{\Psi}_1 &= \varepsilon_1^T \dot{\varepsilon}_1 \\ &= \varepsilon_1^T ((s_2 - \alpha_1) + s_2 - \dot{\eta}_d) \\ &= \varepsilon_1^T ((s_2 - \alpha_1) - c_1 \varepsilon_1) \\ &= -c_1 \varepsilon_1^T \varepsilon_1 + \varepsilon_1^T (s_2 - \alpha_1)\end{aligned}\quad (13)$$

Once the $s_2 - \alpha_1$ is bounded, one obtains

$$\begin{aligned}\dot{\Psi}_1 &= -c_1 \varepsilon_1^T \varepsilon_1 + \varepsilon_1^T (s_2 - \alpha_1) \\ &\leq -c_1 \varepsilon_1^T \varepsilon_1 + \frac{1}{2} \varepsilon_1^T \varepsilon_1 + \frac{1}{2} \omega^2 \\ &\leq -\left(c_1 - \frac{1}{2}\right) \varepsilon_1^T \varepsilon_1 + \frac{1}{2} \omega^2\end{aligned}\quad (14)$$

where $\|s_2 - \alpha_1\| \leq \omega$. Thus, the tracking error of the attitude will be upper bounded if $s_2 - \alpha_1$ is bounded.

Step 2: Design the discrete controller for the second equation in (10).

The following assumptions need to be defined [20-21].

Assumption 2: The partial derivative of $\Upsilon(s_2(\sigma), \tau(\sigma), d(\sigma))$ with respect to $\tau(\sigma)$ is continuous.

Assumption 3: Lipschitz condition is satisfied with (10), which means that

$$\|\Delta s_2(\sigma + 1)\| \leq b \|\Delta \tau(\sigma)\| \quad (15)$$

for any time σ and $\Delta \tau(\sigma) \neq 0$, where $\Delta s_2(\sigma + 1) = s_2(\sigma + 1) - s_2(\sigma)$, $\Delta \tau(\sigma) = \tau(\sigma) - \tau(\sigma - 1)$, b is an positive constant.

If the Assumptions 2-3 are all satisfied, when $\Delta \tau(\sigma) \neq 0$, the model in (10) can be represented by the compact form dynamic linearization (CFDL) data model as follows [20-21]:

$$s_2(\sigma + 1) = s_2(\sigma) + \Theta(\sigma) \Delta \tau(\sigma) \quad (16)$$

where $\Theta(\sigma) = \begin{bmatrix} \theta_{11} & \theta_{12} & \theta_{13} \\ \theta_{21} & \theta_{22} & \theta_{23} \\ \theta_{31} & \theta_{32} & \theta_{33} \end{bmatrix}$ implies the Pseudo Jacobian Matrix.

To evaluate the matrix $\Theta(\sigma)$, the cost index function is established as

$$\begin{aligned}J(\hat{\Theta}(\sigma)) &= \left\| s_2(\sigma) - s_2(\sigma - 1) - \hat{\Theta}(\sigma) \Delta \tau(\sigma - 1) \right\|^2 \\ &\quad + \mu \left\| \hat{\Theta}(\sigma) - \hat{\Theta}(\sigma - 1) \right\|^2\end{aligned}\quad (17)$$

where μ implies the weight factor utilized to restrict the drastic change of $\hat{\Theta}(\sigma)$. By solving $\partial J(\hat{\Theta}(\sigma))/\partial \hat{\Theta}(\sigma) = 0$, it can be obtained that

$$\begin{aligned}\hat{\Theta}(\sigma) &= \rho_1 \left(\Delta s_2(\sigma) - \hat{\Theta}(\sigma - 1) \Delta \tau(\sigma - 1) \right) \Delta \tau^T(\sigma - 1) \\ &\quad \times \left(\Delta \tau(\sigma - 1) \Delta \tau^T(\sigma - 1) + \mu I_{3 \times 3} \right)^{-1} + \hat{\Theta}(\sigma - 1)\end{aligned}\quad (18)$$

where ρ_1 implies a scale factor.

If one of the conditions $\hat{\theta}_{ij}(\sigma) < \underline{\theta}$, $\hat{\theta}_{ij}(\sigma) > \bar{\theta}$, and $\text{sign}(\hat{\theta}_{ij}(\sigma)) \neq \text{sign}(\hat{\theta}_{ij}(1))$ is satisfied, where $\underline{\theta}$ and $\bar{\theta}$ represent the boundaries of $\hat{\theta}_{ij}(\sigma)$, let $\hat{\theta}_{ij}(\sigma) = \hat{\theta}_{ij}(1)$,

The performance index function for the control input is designed as

$$\begin{aligned}J(\tau(\sigma)) &= \|s_2(\sigma + 1) - \alpha(\sigma + 1)\|^2 + \lambda \|\tau(\sigma) - \tau(\sigma - 1)\|^2 \\ &\quad + \|s_2(\sigma + 1) - \alpha(\sigma + 1) - (s_2(\sigma) - \alpha(\sigma))\|^2\end{aligned}\quad (19)$$

where $\lambda > 0$ means the weight factor for the penalty of input variation. By solving $\partial J(\tau(\sigma))/\partial \tau(\sigma) = 0$, the control input is designed as

$$\begin{aligned}\tau(\sigma) &= \rho_2 \left(\lambda I_{3 \times 3} + 2\Theta^T(\sigma)\Theta(\sigma) \right)^{-1} \Theta^T(\sigma) \\ &\quad \left(\alpha(\sigma + 1) - s_2(\sigma) \right) + \rho_3 \left(\lambda I_{3 \times 3} + 2\Theta^T(\sigma)\Theta(\sigma) \right)^{-1} \\ &\quad \Theta^T(\sigma) \left(\alpha(\sigma + 1) - s_2(\sigma) - (\alpha(\sigma) - s_2(\sigma - 1)) \right) + \\ &\quad \rho_4 \left(\lambda I_{3 \times 3} + 2\Theta^T(\sigma)\Theta(\sigma) \right)^{-1} \Theta^T(\sigma) \Theta(\sigma - 1) \\ &\quad \left(\tau(\sigma - 1) - \tau(\sigma - 2) \right) + \tau(\sigma - 1)\end{aligned}\quad (20)$$

where ρ_2 , ρ_3 , and ρ_4 are scale factors.

C. Tent Map-Based Pigeon-Inspired Optimization

Original PIO is proposed by Duan and Qiao in [17], and the specific mathematical model is described in the following part.

Firstly, initialize the pigeon swarm parameters. The swarm size is set as N_p , and the maximum iterations of different stages are $N_{c1 \max}$ and $N_{c2 \max}$, respectively. Select the appropriate ranges $[X_{\max}, X_{\min}]$ for the parameters to be optimized in the filter and the controller, where $X_{\max} \in \mathbb{R}^n$ and $X_{\min} \in \mathbb{R}^n$ are upper and lower boundaries, n is the number of the parameters. i_{th} pigeon is initialized with the position X_0^i and the velocity V_0^i .

Secondly, the map and compass operator is designed as

$$\begin{cases} V_l^i = V_{l-1}^i \cdot e^{-Rl} + r_1 \cdot (X_g - X_l^i) \\ X_l^i = X_{l-1}^i + V_l^i \end{cases} \quad (21)$$

where l implies the iteration number, R means the map and compass factor, $0 < r_1 < 1$ represents a random number, V_l^i and X_l^i are velocity and position of i_{th} pigeon in l_{th} iteration.

Thirdly, the landmark operator is described as

$$\begin{cases} X_l^i = X_{l-1}^i + r_2 \cdot (X_l^c - X_{l-1}^i) \\ X_l^c = \frac{\sum_{i=1}^{N_p(l)} X_l^i f(X_l^i)}{N(l) \cdot \sum_{i=1}^{N_p(l)} f(X_l^i)} \\ N(l) = \text{ceil} \left(\frac{N(l-1)}{2} \right) \end{cases} \quad (22)$$

where $0 < r_2 < 1$ represents a random number, X_l^c is the center of the pigeons in l_{th} iteration, $N(l)$ is the number of pigeons, $f(X_l^i)$ means the fitness of the X_l^i , $\text{ceil}()$ is rounded up function.

However, the pigeon swarm suffers the problem that falls into the local optimum for its fast convergence rate. TMPIO is developed to alleviate the premature convergence of PIO. The TMPIO fuses the two stages into one operator as

follows:

$$\begin{cases} V_{l'}^i = V_{l-1}^i \cdot e^{-Rl} + r_1 \cdot (X_g - X_l^i) \\ V_{l''}^i = V_{l-1}^i \cdot e^{-Rl} + r_1 \cdot (X_g - X_l^i) + h_l \cdot (X_l^c - X_{l-1}^i) \\ Y_1^i = X_{l-1}^i + V_{l'}^i \\ Y_2^i = X_{l-1}^i + V_{l''}^i \\ X_l^i = \begin{cases} Y_1^i, & \text{if } f(Y_1^i) \geq f(Y_2^i) \\ Y_2^i, & \text{if } f(Y_1^i) < f(Y_2^i) \end{cases} \\ V_l^i = \begin{cases} V_{l'}^i, & \text{if } f(Y_1^i) \geq f(Y_2^i) \\ V_{l''}^i, & \text{if } f(Y_1^i) < f(Y_2^i) \end{cases} \\ X_l^c = \frac{\sum_{i=1}^{N_p} X_l^i \cdot f(X_l^i)}{N_p \cdot \sum_{i=1}^{N_p} f(X_l^i)} \end{cases} \quad (23)$$

where h_l is generated by Tent map. The update rule of h_l is

$$h_{l+1} = \begin{cases} 2h_l & 0 \leq h_l \leq 0.5 \\ 2h_l - 1 & 0.5 < h_l \leq 1 \end{cases} \quad (24)$$

h_0 is initialized with a random number within (0,1).

Halving the number of pigeons in the landmark stage is cancelled to slow down the convergence rate in TMPIO. Meanwhile, the landmark operator is used as a mutated function with Temp map as the coefficient, which makes the pigeons have a greater ability to escape from the local optimum.

The structure of using TMPIO to optimize the controller is illustrated in Fig. 1. $\gamma_1, \gamma_2, \chi_1, \chi_2$ in the filter and $c_1, \rho_1, \rho_2, \rho_3, \rho_4, \mu, \lambda$ in MFAC influencing the tracking performance need to be optimized. The integral of time-weighted absolute value of the error (ITAE) [22] is selected as cost function, given by

$$J = \int_0^{\infty} t \|\varepsilon_1\| dt \quad (25)$$

and the fitness function is defined as the reciprocal of the cost function.

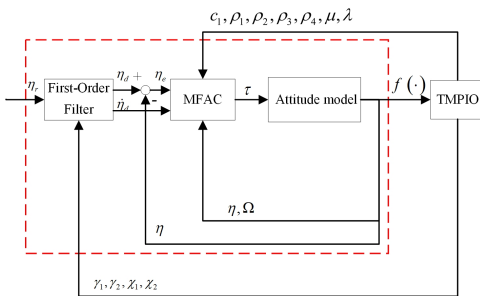


Fig. 1: Structure of using TMPIO to optimize the controller.

IV. SIMULATION RESULTS

The attitude model parameters of the quadrotor are set as follows: $J = \text{diag}\{0.16, 0.3, 0.31\} \text{kg} \cdot \text{m}^2$, $d = [0.1 \cos(0.2t), 0.1 \cos(0.4t), 0.1 \cos(0.2t)]^T$. The initial angle and angular velocity are all zero vector. The reference signal is set as $\eta_r = [0.2, 0.2, 0.2]^T \text{rad}$.

To verify the advantages of the TMPIO, original PIO, genetic algorithm (GA), and particle swarm optimization (PSO)

TABLE I: Parameters of The Methods

Algorithm	Variable	Description	Value
PIO/TMPIO	R	Map and compass factor	0.02
	P_c	Crossover probability	0.9
GA	P_m	Mutation probability	0.1
	w	Inertial weight	0.8
PSO	l_1	Learning factor-cognitive constant	1.3
	l_2	Learning factor-social constant	1.5

are selected for the comparison simulation. The parameters of the methods are given in Table I.

The maximum iteration of GA, PSO and TMPIO is 100, and the maximum iteration in different stages for PIO is 90 and 10, respectively.

The evolution curves of cost value are described in Fig. 2. Since the cost value is small, the vertical axis uses the $\log()$ function for the better display effect. GA, PIO, PSO and TMPIO have the final cost value of 0.0684, 0.0458, 0.0456 and 0.0443. GA has the worst optimization performance for the established model. PIO, PSO and TMPIO have faster convergence rate than GA. TMPIO reached the minimal cost value at 15th iteration, while the iteration of GA, PIO and PSO are 63, 28, and 74. Thus, TMPIO has the advantages in both convergence rate and optimization ability than other three optimization algorithms.

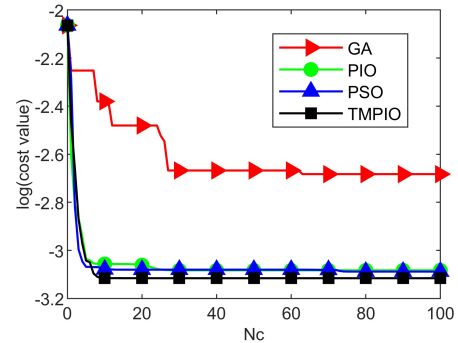


Fig. 2: Cost value evolutionary curves.

The simulation results of MFAC controller with optimized parameters by TMPIO are shown in Fig. 3. Three channels of the Euler angle track the reference signal with small overshoots within 1 second, which means that the control performance can be achieved in the case of unknown model parameters and external disturbance with the proposed MFAC method.

To further illustrate the effectiveness of the proposed controller, gust wind is added to the disturbance, given as $d = [0.5 + 0.1 \cos(0.2t), 0.5 + 0.1 \cos(0.4t), 0.3 + 0.1 \cos(0.2t)]^T$. The time varying reference signal is set as $\eta_r = [0.2 \cos(0.5t), 0.3 \cos(0.5t), 0.15 \cos(0.5t)]^T$. The simulation results are presented in Fig. 4. The attitude of the quadrotor controlled by MFAC can precisely track the time varying reference signal with gust wind.

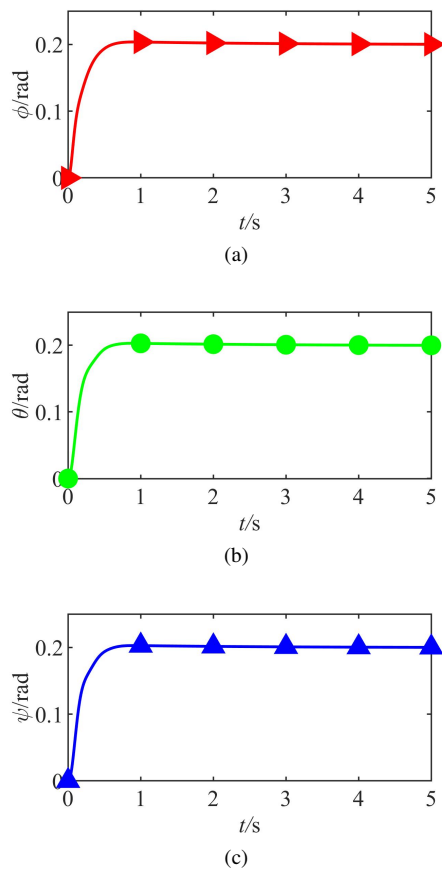


Fig. 3: Attitude curves with optimized parameters in case 1. (a) ϕ . (b) θ . (c) ψ .

V. CONCLUSION

A novel PIO variant is proposed to optimize the model-free controller for the quadrotor attitude control problem in this paper. For the outer-loop of the attitude model, the idea of the backstepping control is utilized to maintain the stability. For the inner-loop with unknown model parameters and external disturbance, the dynamic linearization method is applied to obtain discrete model, and a differential term is added in the performance index function of the control input. The feasibility of the controller and the advantages of TMPIO are verified by the simulation results.

REFERENCES

- [1] H. Duan and Y. Yuan, "Active disturbance rejection attitude control of unmanned quadrotor via paired coevolution pigeon-inspired optimization", *Aircr. Eng. Aerosp. Technol.*, vol. 94, no. 2, pp. 302-314, 2022.
- [2] M. Tao, Q. Chen, X. He, and S. Xie, "Fixed-time filtered adaptive parameter estimation and attitude control for quadrotor UAVs", *IEEE Trans. Aerosp. Electron. Syst.*, vol. 58, no. 5, pp. 4135-4146, Oct. 2022.
- [3] S. Nadda and A. Swarup, "Improved quadrotor altitude control design using second-order sliding mode", *J. Aerospace Eng.*, vol. 30, no. 6, Nov. 2017, Art. no. 04017065.
- [4] M. Culter and P. H. Jonathan, "Analysis and control of a variable-pitch quadrotor for agile flight", *J. Dyn. Syst. Meas. Control*, vol. 137, no. 10, Oct. 2015, Art. no. 1010,

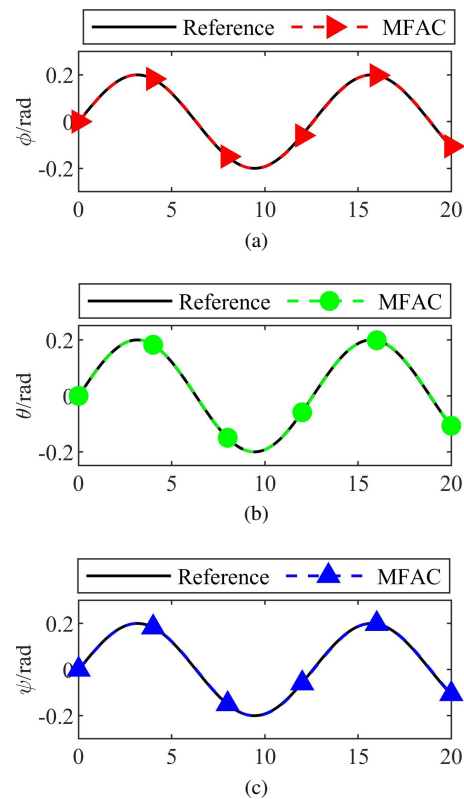


Fig. 4: Attitude curves with optimized parameters in case 2. (a) ϕ . (b) θ . (c) ψ .

- [5] K. Liu and R. J. Wang, "Antisaturation command filtered backstepping control-based disturbance rejection for a quadrotor UAV", *IEEE Trans. Circuits Syst. II Express Briefs*, vol. 68, no. 12, pp. 3577-3581, Dec. 2022.
- [6] J. X. Dou and B. C. Wen, "An adaptive robust attitude tracking control of quadrotor UAV with the modified Rodrigues parameter", *Meas. Control*, vol. 55, no. 9-10, pp. 1167-1179, Nov. 2022.
- [7] M. Labbadi and M. Cherkaoui, "Robust adaptive backstepping fast terminal sliding mode controller for uncertain quadrotor UAV", *Aerosp. Sci. Technol.*, vol. 93, Oct. 2019, Art. no. 105306.
- [8] B. Li and Y. X. Wang, "An enhanced model predictive controller for quadrotor attitude quick adjustment with input constraints and disturbances", *Int. J. Control Autom. Syst.*, vol. 20, no. 2, pp. 648-659, Feb. 2022.
- [9] S. Harshavarthini, R. Sakthivel, and C. K. Ahn, "Finite-time reliable attitude tracking control design for nonlinear quadrotor model with actuator faults", *Nonlinear Dyn.*, vol. 96, no. 4, pp. 2681-2692, Jun. 2019.
- [10] S. Harshavarthini, S. Selvi, R. Sakthivel, and D. J. Almkhles, "Non-fragile fault alarm-based hybrid control for the attitude quadrotor model with actuator saturation", *IEEE Trans. Circuits Syst. II Express Briefs*, vol. 67, no. 11, pp. 2647-2651, Nov. 2020.
- [11] Z. S. Hou, "The parameter identification, adaptive control and model free learning adaptive control for nonlinear systems," Ph.D. dissertation, College Inf. Sci. Eng., Northeastern Univ., Shenyang, China, 1994.
- [12] S. Baldi, D. Sun, X. Xia, G. Zhou, and D. Liu, "Ardupilot-based adaptive autopilot: Architecture and software-in-the-loop experiments", *IEEE Trans. Aerosp. Electron. Syst.*, vol. 58, no. 5, pp. 4473-4485, Oct. 2022.
- [13] S. Liu, Z. Hou, T. Tian, Z. Deng, and Z. Li, "A novel dual successive projection-based model-free adaptive control method and application to an autonomous car", *IEEE Trans. Neural Netw. Learning Syst.*, vol. 30, no. 11, pp. 3444-3457, Nov. 2019.
- [14] S. Zhang, P. Zhou, Y. Xie, and T. Chai, "Improved model-free adaptive predictive control method for direct data-driven control of a wastewater

- treatment process with high performance”, *J. Process Control*, vol. 110, no. 11-23, Feb. 2022.
- [15] H. Gao, G. Ma, Y. Lv, and Y. Guo, “Forecasting-based data-driven model-free adaptive sliding mode attitude control of combined spacecraft”, *Aerosp. Sci. Technol.*, vol. 86, pp. 364-374, Mar. 2019.
- [16] Y. Weng and N. Wang, “SMC-based model-free tracking control of unknown autonomous surface vehicles”, *ISA Trans.*, vol. 130, pp. 684-691, Nov. 2022.
- [17] H. B. Duan and P. X. Qiao, “Pigeon-inspired optimization: A new swarm intelligence optimizer for air robot path planning”, *Int. J. Intell. Comput. Cybern.*, vol. 7, no. 1, pp. 24-37, Mar. 2014.
- [18] Z. Y. Yang, H. B. Duan, Y. M. Fan, and Y. M. Deng, “Automatic carrier landing system multilayer parameter design based on Cauchy mutation pigeon-inspired optimization”, *Aerosp. Sci. Technol.*, vol. 79, pp. 518-530. Aug. 2018.
- [19] Z. Guan, H. Liu, Z. Zheng, M. Lungu, and Y. Ma, “Fixed-time control for automatic carrier landing with disturbance”, *Aerosp. Sci. Technol.*, vol. 108, Jan. 2021, Art. no. 106403.
- [20] Z. Hou and S. Jin, *Model Free Adaptive Control: Theory and Applications*. Boca Raton, FL, USA: CRC Press, 2013.
- [21] Z. Hou and S. Jin, “Data-driven model-free adaptive control for a class of MIMO nonlinear discrete-time systems”, *IEEE Trans. Neural Netw.*, vol. 22, no. 12, pp. 2173-2188, Dec. 2011.
- [22] Q. Yang, W. N. Chen, J. D. Deng, Y. Li, T. Gu and J. Zhang, “A level-based learning swarm optimizer for large-scale optimization”, *IEEE Trans. Evol. Comput.*, vol. 22, no. 4, pp. 578-594, Oct. 2018.